04,08

Identification of paramagnetic centers of gadolinium and iron in scandium and yttrium orthosilicates

© V.A. Vazhenin[1], A.P. Potapov[1], K.A. Subbotin[2,3], A.V. Fokin[1], M.Yu. Artyomov[1], A.I. Titov[2,3], S.K. Pavlov[2,3]

[1] Institute of Natural Sciences and Mathematics,
Ural Federal University named after the First President of Russia B.N. Yeltsin
Yekaterinburg, Russia
[2] Prokhorov Institute of General Physics, Russian Academy of Sciences,
Moscow, Russia
[3] Mendeleev University of Chemical Technology,
Moscow, Russia

E-mail: vladimir.vazhenin@urfu.ru

Received March 27, 2023
Revised March 27, 2023
Accepted March 28, 2023

The study of grown $Sc_2SiO_5:Gd$ and $Sc_2SiO_5:Fe$ crystals was carried out by the paramagnetic resonance method. It has been established that Fe^{3+} ions replace Sc^{3+} in both crystallographic positions, while Gd^{3+} ions exhibit a single center localized in a larger position with a coordination number of 7. Measurement of the orientational behavior of the positions of transitions of Fe^{3+} and Gd^{3+} centers in two orthogonal planes made it possible to determine the parameters of their triclinic spin Hamiltonians. To determine the localization of impurity ions Cr^{3+}, Fe^{3+} and Gd^{3+} in scandium and yttrium silicates, the orientation of the main Z axes of the fine structure tensors of the second rank was used.

Keywords: scandium and yttrium silicates, impurity ions, paramagnetic resonance.

DOI: 10.21883/PSS.2023.05.56045.45

1. Introduction

For development of quantum electronics, quantum cybernetics, scintillator materials, etc., capability of determining concentrations and charge states of uncontrolled impurities is essential. Electron paramagnetic resonance (EPR) is one of the most informative electronic-level detection methods of transition and rare-earth elements in crystals [1]. This is, in particular, applicable to iron(II) and iron(III) ions which are the most important accidental impurities in many crystals that degrade their characteristics. To implement such diagnostic functions, valid information about EPR spectra of impurity centers in crystals essential for the above mentioned applications.

Isostructural yttrium and scandium orthosilicate crystals are exactly such materials. Y_2SiO_5 doped with chromium ions is studied as active medium for solid-state lasers generating the near IR emission [2] and as passive laser q-switch [3]. Sc_2SiO_5 single-crystals with rare earth impurity (Tm^{3+}, Ho^{3+}, Nd^{3+}) attract attention due to their potential use in solid-state lasers [4,5]. Rare earth impurity ions with nuclear spin, in particular in yttrium silicate [6], are studied as a possible basis for quantum memory implementation in the optical range.

$Y_2SiO_5:Cr$ crystals were studied using the EPR method by authors of [7] who found that the observed spectrum was associated with Cr^{4+} with electronic spin $S = 1$ localized in tetrahedral position of silicon. EPR spectra of chromium-doped scandium and yttrium orthosilicates are studied in [8]. Two different triclinic Cr^{3+} centers with spin $S = 3/2$ localized in nonequivalent (6- and 7-coordinated) scandium positions were found and studied in Sc_2SiO_5. In Y_2SiO_5 crystal, only one center with a spectrum identical to the spectrum observed in [7] was detected. Studies [8,9] definitely show that this center is attributable to Cr^{3+} in one of the two nonequivalent yttrium positions, rather than to Cr^{4+} in the silicon position as was believed in [7]. Signals of the second Cr^{3+} center in Y_2SiO_5 with two orders of magnitude lower intensity that the first center signals were recorded in a specially grown crystal with odd ^{53}Cr isotope in [10]. This center is attributable to Cr^{3+} localization in other yttrium position in the crystal. Both crystals studied in [8,10] had numerous weak signals not identified at that stage.

Besides iron, commercial yttrium- and scandium-containing reagents and, therefore, single-crystals grown from them are known to often contain trace quantities of rare-earth ions (due to their similar chemical properties) that substitute these pseudo-rare-earth ions in crystal structures, but their EPR spectra, excluding Gd^{3+} and Eu^{2+}, are not observed at room temperature. Actually, the authors of [11], having meticulously studied the mentioned above weak (not belonging to chromium ions) EPR signals of $Y_2SiO_5:^{53}Cr$ crystals investigated in [10], have found that all these signals are attributable to two ions Gd^{3+} localized in two physically nonequivalent yttrium positions (like those in which Cr^{3+} centers are also localized).

Cr^{3+} centers in scandium orthosilicate with chromium impurity were studied in [8,12,13]. All these studies, besides intense Cr^{3+} transitions, detected weaker unknown signals. Thorough analysis of the orientational behavior of the specified signals has shown that part of them corresponds to Gd^{3+} center transitions in the structural localization of single-type Sc^{3+} (see Figure 1 in [13]). The absence of visible signals from the gadolinium center in another scandium position could be associated with its lower intensity against the background of numerous non-identified signals, among which, in particular, transitions of uncontrolled iron(III) impurity are possible. Moreover, the second Gd^{3+} center could be masked by intense Cr^{3+} signals.

For reliable identification of uncontrolled impurities in this crystal, Sc_2SiO_5 crystals doped with gadolinium only (electronic configuration $Gd^{3+}-4f^7$, ground state $^8S_{7/2}$) and iron only ($3d^5$, $^6S_{5/2}$ — for Fe^{3+}) were grown for the purpose of this study. EPR investigations of paramagnetic centers implemented in these crystals were carried out.

2. Samples and measurement procedure

$Sc_2SiO_5:Gd$ and $Sc_2SiO_5:Fe$ single-crystals were grown by Czochralski method using „Kristall-2“ (USSR) system. Crystal growing mixtures were prepared from SkO-z OST 48-4-417-87 Sc_2O_3, GdO-g OST 48-200-81 Gd_2O_3 reagents (both reagents — p/o M-5649, USSR) SiO_2 W30 (Wacker Chemie AG, Austria) and ACS 2-4 TU 6-09-1418-78 Fe_2O_3 (Reakhim, USSR). All reagents were classified by purity as at least 4N. The reagents were preliminary dried, accurately weighed on Adventurer AX523 (OHAUS, USA) balance, then the weighed quantities were thoroughly mixed using Multi RS-60 (BioSan, Latvia) mixer. The prepared mixtures were burned in air in EKPS-10/1250 SPU 4107 (Russia) muffle furnace at 700°C during 5 h. Nominal (charge) concentration of Gd_2O_3 in $Sc_2SiO_5:Gd$ crystal was 0.005 wt%, nominal concentration of Fe_2O_3 in $Sc_2SiO_5:Fe$ crystal was 0.1 wt%.

Growing was carried out in an iridic crucible 30 mm in diameter and height in service nitrogen atmosphere (actual residual concentration of oxygen in the growth atmosphere was not measured, but it was max. 1 vol% according to our assessments). Pulling speed at the nominal growth stage was 1 mm/h, rotation speed was 6 rpm. After completion of the growth and separation of the grown boule from the melt mirror, it was cooled down at a rate of 8°C/h to room temperature. After growing, additional annealing of crystals was carried out in air in the muffle furnace at 1000°C during three weeks. Heating/cooling rate was 10°C/h. The grown crystals were transparent and colorless. The crystals were free from growth striation, cracks and other 3D defects.

Structure of Sc_2SiO_5 crystals belongs to a monoclinic crystal system, space group is C_2/c (C_{2h}^6). Lattice constants in cell $I2/c$ are: $a = 0.997$ nm, $b = 0.643$ nm, $c = 1.206$ nm, $\beta = 103.94°$ [14]. All atoms in the structure have a local crystal field symmetry 1 (C_1): silicon is in a distorted oxygen tetrahedron, Sc^{3+} ions occupy two nonequivalent positions with coordination numbers 6 ($M1$) and 7 ($M2$). Each atomic position is multiplied by the cell symmetry elements (inversion center and axis $C_2 \parallel \mathbf{b}$) up to four. In this connection, if the paramagnetic ion is localized in any of the three positions ($M1$, $M2$, Si), two magnetically nonequivalent spectra will be observed in EPR. And when magnetic field induction vector **B** is in lattice plane **ac** or parallel to crystallographic axis **b**, then these two spectra become equivalent.

Crystal orientation against the optical indicatrix axes (one of which coincides with crystallographic axis **b**, and other two are in lattice plane **ac** being rotated about axes **a** and **c** at an angle depending on the wavelength) was carried out by crystallooptic methods using „Biomed-5“ (PRC) microscope. Orientation error was max. 1°. After orientation, samples for EPR measurements were cut in the form of cubes with side equal to 6 mm. Cube faces were parallel to the optical indicatrix axes.

The orientation behavior of the EPR spectra at room temperature was measured on a EMX Plus Bruker X-band spectrometer in fields up to 1.5 T. The samples in the spectrometer resonant cavity were attached to a holder secured on the rod of the standard automatic goniometer and capable of rotating about the axis perpendicular to the rod.

3. Gd^{3+} centers in scandium orthosilicate

EPR spectra of gadolinium-doped Sc_2SiO_5 samples measured with magnetic field rotation in two orthogonal planes have shown the presence of only one Gd^{3+} center represented by two magnetic nonequivalent spectra. Figure 1 clearly shows that almost all signals in the scandium orthosilicate belong to a single Gd^{3+} center (see Introduction) observed in [13].

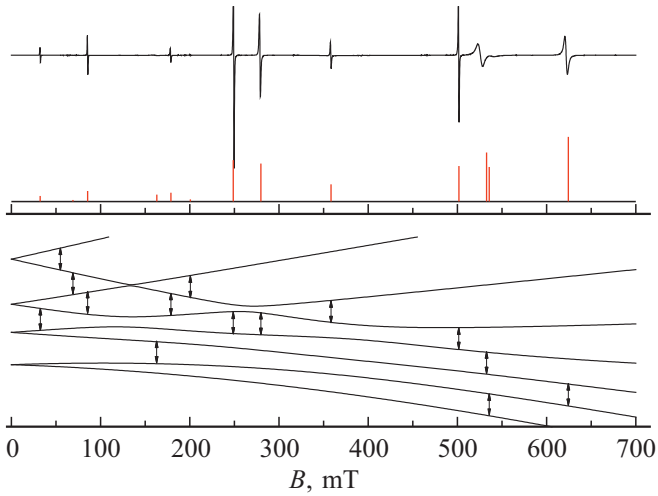

Figure 1. Experimental EPR spectrum, energy levels, calculated positions and integral intensities of Gd^{3+} center transitions in Sc_2SiO_5 at **B** ∥ **b** and 9836 MHz.

Table 1. SH parameters of Gd^{3+} center in Sc_2SiO_5 at room temperature in coordinate system $\mathbf{z} \parallel \mathbf{b}$ and in the principal axes of the second-rank fine structure tensor. b_{nm}, c_{nm} and rms deviation F(N) — in MHz; N is the number of transition positions used in the optimization procedure. Double signs of b_{nm} and c_{nm} with odd projections correspond to magnetic nonequivalent spectra of one center (see Section 2). Absolute signs were not determined.

Parameters	$\mathbf{z} \parallel \mathbf{b}$ (herein)	In principal axes (herein)	$\mathbf{z} \parallel \mathbf{b}$ [13]	In principal axes [13]
g	1.990	1.990	1.990	1.990
b_{20}	2880	3510	2860	3480
b_{21}	±5500	0	±5430	0
b_{22}	2900	2470	2880	2470
c_{21}	±2980	0	±3200	0
c_{22}	100	0	160	0
b_{40}	10	10	6	0
b_{41}	±80	5	∓60	40
b_{42}	40	−20	45	15
b_{43}	∓50	100	±10	110
b_{44}	−15	15	15	40
c_{41}	∓50	90	±40	40
c_{42}	−20	10	−10	−30
c_{43}	±5	90	∓100	−370
c_{44}	−60	−50	85	60
F(N)	47(588)		60(438)	

A laboratory coordinate system introduced in [13] was used for system description: $\mathbf{z} \parallel \mathbf{b}$, axis $\mathbf{x}$ is spaced away from axis $\mathbf{c}$ by 6°. Spin Hamiltonian (SH) for electronic spin $S = 7/2$ is as follows [15]:

$$H_{\text{sp}} = \beta(\mathbf{BgS}) + \frac{1}{3}\sum_m (b_{2m}O_{2m} + c_{2m}\Omega_{2m}) + \frac{1}{60}\sum_m (b_{4m}O_{4m} + c_{4m}\Omega_{4m}) + \frac{1}{1260}\sum_m (b_{6m}O_{6m} + c_{6m}\Omega_{6m}), \quad (1)$$

where g is g-factor, β is Bohr magneton, O_{nm}, Ω_{nm} are Stevens spin operators, b_{nm}, c_{nm} are fine structure parameters.

Orientational behavior (azimuthal — in plane **ac** and polar — in the orthogonal plane containing axis **z**) of EPR positions of Gd^{3+} signals is shown in Figure 2, 3. Double experimental dots on the azimuthal dependence (Figure 2) are attributable to splitting due to magnetic field exit from plane **ac** not exceeding one degree, according to our estimate, the SH optimization procedure in this case used average values.

The SH optimization was preceded by the identification of the transition level numbers for the observed dependences, the identification procedure details are describe in [11]. SH parameters listed in Table 1 were calculated by minimization of rms deviation of the calculated resonance frequencies (by an eighth-order complex matrix diagonalization) from the measured resonance transition frequencies. Consideration of the sixth-rank parameters introduced little improvement to the spectrum descriptions. The same Table lists the SH parameters of Gd^{3+} center in the local coordinate system XYZ of the second-rank fine structure tensor that becomes diagonal with $|b_{20}| > |b_{22}|$. The direction cosine matrix that couples two coordinate systems is as follows:

	X	Y	Z
x	−0.9300	0.0923	0.3558
y	−0.0460	−0.9896	0.1364
z	0.3647	0.1105	0.9246

The second-rank parameters achieved herein are fairly in line with the results of [13], while the apparent difference of two second-rank parameter sets (up to signs, Table 1) is indicative of low accuracy that prevents the analysis of their principal axes system.

Thus, in gadolinium-doped Sc_2SiO_5, only one Gd^{3+} center is observed which in line with [13]. If any second center exists, then its concentration is several orders lower than that of the first one. The described center is more likely associated with Gd^{3+} (ionic radius $R_i = 0.938$ Å [16]) localized in more spacious scandium position *M2* with seven-fold oxygen environment and $R_i > 0.745$ Å [16]. The principal axis of the center Z, according to the direction cosine matrix, is spaced away from **b** at $\sim 22°$ ($\arccos 0.9246$), while in Y_2SiO_5 according to [11], two Gd^{3+} centers (Gd 1 and Gd 2) are observed with axes in local coordinate systems rotated at $\sim 66°$ (Gd 1) and $\sim 19°$ (Gd 2) about crystallographic axis **b**.

Taking into account the proximity of the principal axis deviation of center Gd 2 in the yttrium silicate to the similar value for a single gadolinium center found in the scandium

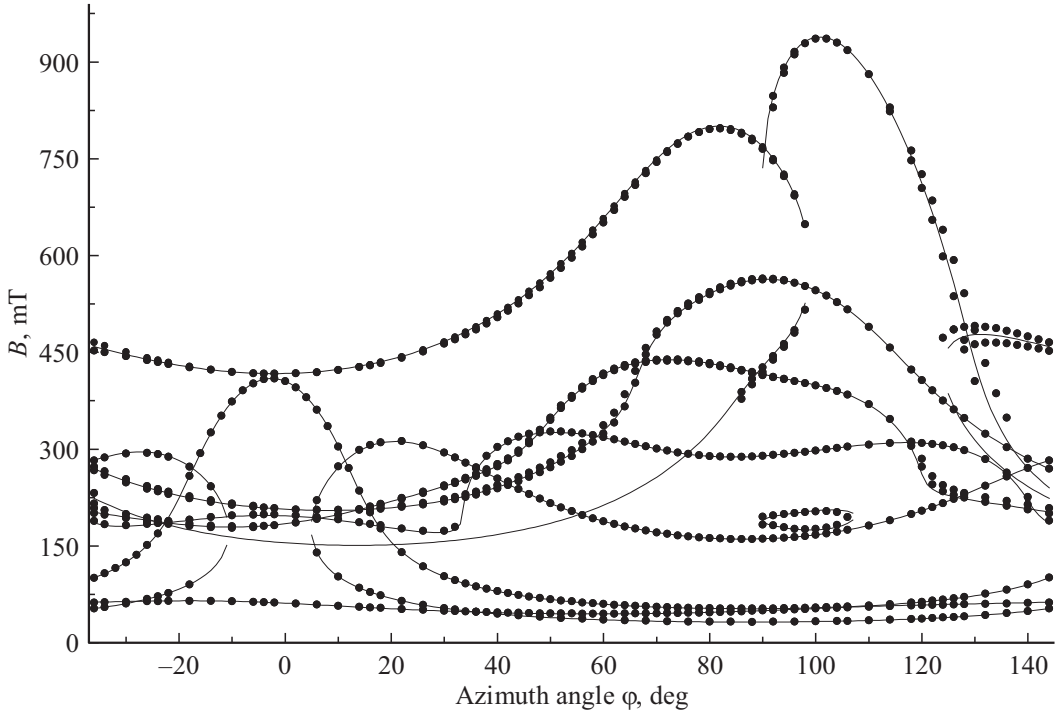

Figure 2. Azimuthal angular dependence of transition positions of Gd^{3+} center in Sc_2SiO_5 at 9827 MHz. Curves — are the result of dependence calculations with parameters from Table 1.

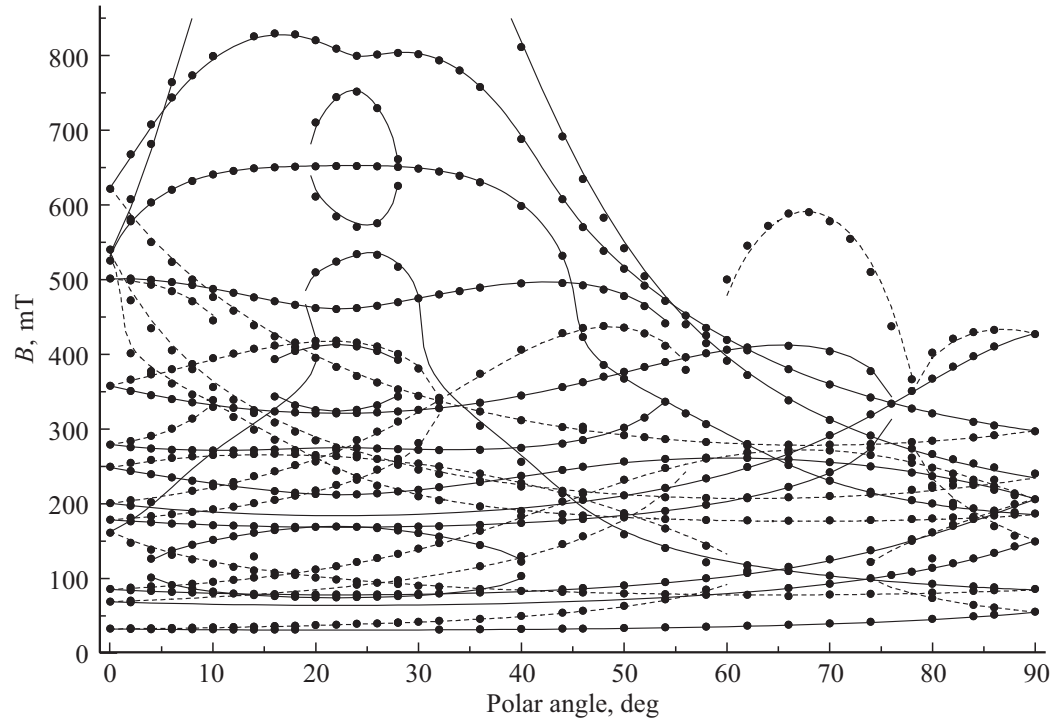

Figure 3. Polar angular dependence of EPR transition positions of Gd^{3+} center in Sc_2SiO_5 at 9835 MHz at $\varphi = 14^\circ$ (Figure 2). Curves — are the result of dependence calculations with parameters from Table 1. Solid and dashed curves correspond to two gadolinium ions in magnetic nonequivalent positions coupled by C_2 operation.

silicate, it would be reasonable to assume that it is Gd 2 that is localized in the yttrium position ($R_i = 0.96$ Å [16]) with coordination number 7. It should be noted that concentration of Gd 2 centers in Y_2SiO_5 resulting from signal intensities is approximately three times higher than that of Gd 1.

Other situation in the discussed silicates occurs for odd isotope of $^{143}Nd^{3+}$ rare-earth ion ($R_i = 0.983$ Å [16]). Both in Y_2SiO_5 ($g_z = 4.1038$) [17,18] and in Sc_2SiO_5 ($g_z = 3.48$) [19], only one $^{143}Nd^{3+}$ center is observed. The modulation envelope analysis in [20] carried out by three-pulse electron spin echo procedure on samples with ^{28}Si isotope has found that $^{143}Nd^{3+}$ center in Y_2SiO_5 was attributable to the neodymium ion in the yttrium position with seven-fold oxygen environment. It would be reasonable to assume that the same position Y^{3+} in the yttrium silicate will be occupied by Gd 2 center with more intense EPR spectrum having ionic radius 1.0 Å in the seven-fold environment [16].

It is important that in previous study [21] in the EPR spectrum of neodymium-doped Y_2SiO_5 crystal, two centers with $g_{max} = 3.825$ and $g_{max} = 4.171$ were observed and were assigned by the authors to Nd^{3+} localized in two physically nonequivalent yttrium positions. Similar spectrum pairs were found in the yttrium silicate crystals with Ce^{3+}, Yb^{3+} and Er^{3+} rare-earth ion impurities [21]. Difference in the number of paramagnetic rare-earth centers detected in Y_2SiO_5 is likely associated with different crystal growing methods and conditions.

4. Fe^{3+} centers in scandium orthosilicate

The EPR spectrum of iron-doped Sc_2SiO_5 demonstrates at room temperature transitions of two Fe^{3+} centers (Fe 1 and Fe 2) naturally localized in two different scandium positions. Signals of one Gd^{3+} center similar to those described in Section 3 and numerous weak signals identified as belonging to a accidental manganese impurity with nuclear spin 5/2 (Mn^{2+}, S = 5/2 or/and Mn^{4+}, S = 3/2) were also detected. Large amount of manganese ions may be associated with their entrance in scandium positions of both types as well as in silicon positions. For example, in [22], manganese ions in $Y_3Al_5O_{12}$ garnet crystal were found in all three types of cation positions in this crystal.

Unidentified signals are also present in the EPR spectrum of the studied Sc_2SiO_5 : Fe crystal. Figure 4 shows the spectrum of this crystal in the magnetic field whose vector **B** is slightly out of plane **ac**. This is supported by splitting of Fe 2 center signal in $\sim$ 540 mT field, while other transitions of magnetic nonequivalent centers are collected together. Wide lines at 350 and 900 mT are attributable to the sample holder and air oxygen, respectively. The most intense manganese signals are located near 250 mT.

Orientational behavior of the experimental positions of Fe 1 and Fe 2 center positions in two planes is shown in Figure 5–6. As in case of gadolinium centers (see

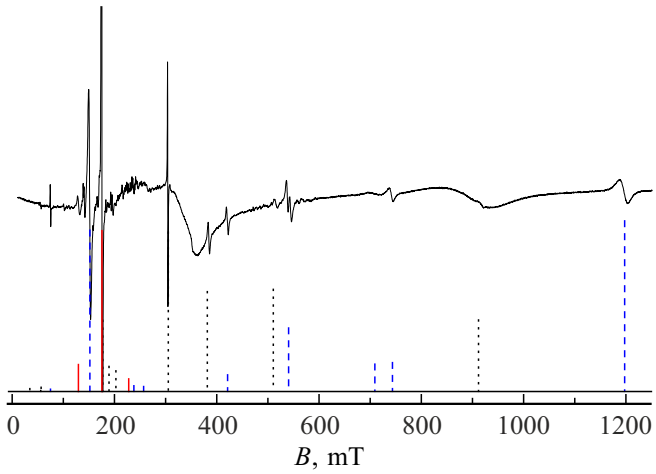

Figure 4. The EPR spectrum of Sc_2SiO_5 : Fe crystal at 9822 MHz in magnetic field orientation $\theta \approx 90°$, $\varphi = 107°$ of the laboratory coordinate system. Vertical sections (red solid lines for Fe 1, blue dashed lines for Fe 2, black dotted line for Gd^{3+}) show calculated positions and transition integral intensities.

Section 3), many signals on the azimuthal dependence are split (double dots in Figure 5) due to magnetic field deviation from plane **ac**. Splitting is especially large for transition $5 \leftrightarrow 6$ of Fe 2 center at $\varphi \sim -45°$ shown with arrow in Figure 5. However, the polar angular dependence calculation at this φ has shown that splitting of this type occurs when the magnetic field deviates from plane **ac** by only $\sim 1.5°$. It should be noted that splitting is predicted to be apparently nonsymmetric and, therefore, the use of the mean of two resonance positions to determine SH parameters is not desirable.

The absence of signals in the polar dependence (Figure 6) at $\mathbf{B} \parallel \mathbf{b}$ in the fields much higher than 400 mT seems to contradict with the electronic state structure and predicted transitions in Figure 7. However, as can be seen, two transitions $3 \leftrightarrow 4$ of Fe 2 center are predicted near the minimum distance between the energy levels of these transitions, i.e. between almost parallel levels (Figure 7). This shall result and actually results in large signal spreading and, therefore, in low accuracy of resonance position determination. Similar situation occur with transitions $4 \leftrightarrow 5$ of center Fe 2. Minimum energy difference of states 2 and 3 of Fe 2 center at $\mathbf{B} \parallel \mathbf{b}$ above 800 mT is higher than the operating frequency of the spectrometer, but becomes lower at $\theta \geq 1°$ and owing to this one of the two transitions is detected.

The identification of experimental dependence transitions in Figure 5–6 carried out according to procedure [11] allowed for the optimization of the spin Hamiltonian parameters (expression 1 without sixth rank) of two Fe^{3+} centers without using azimuthal dependences with large signal splitting of magnetic nonequivalent spectra. The results are shown in Table 2.

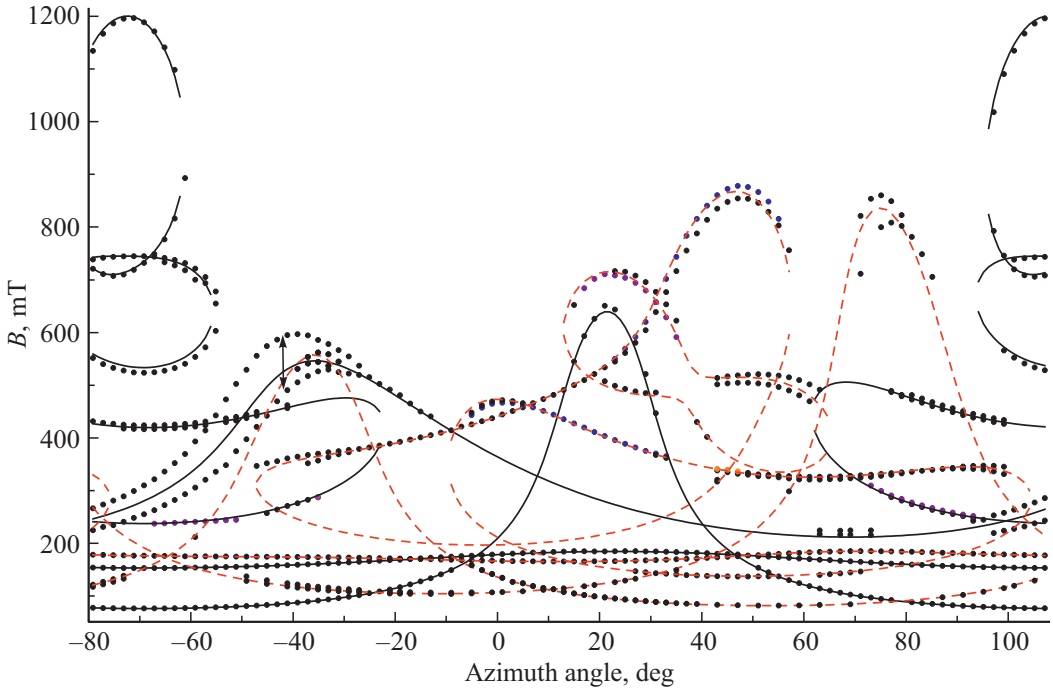

Figure 5. Azimuthal angular dependence of transition positions of Fe 1 centers (red dashed lines) and Fe 2 (black solid lines) in Sc_2SiO_5 at 9827 MHz. Curves — are the result of dependence calculations with parameters from Table 2.

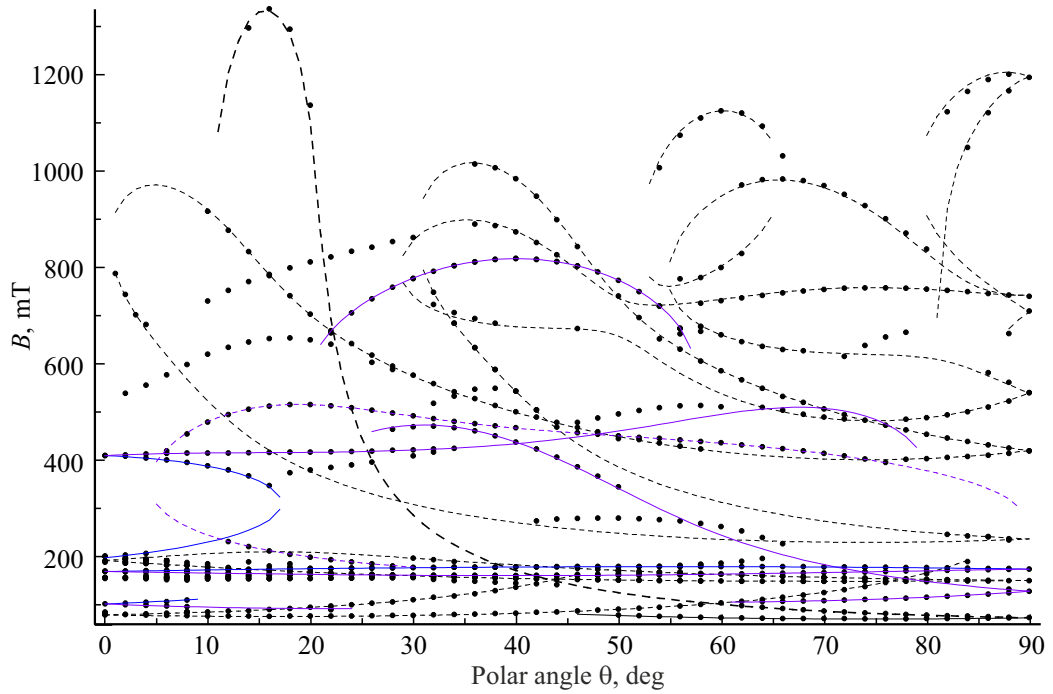

Figure 6. Polar angular dependence of transition positions of Fe 1 centers (blue solid lines) and Fe 2 (black dashed lines) in Sc_2SiO_5 : Fe at 9827 MHz with $\varphi = 107°$. Curves — are the result of dependence calculations with parameters from Table 2. Dots without curves — are the signals of unidentified centers.

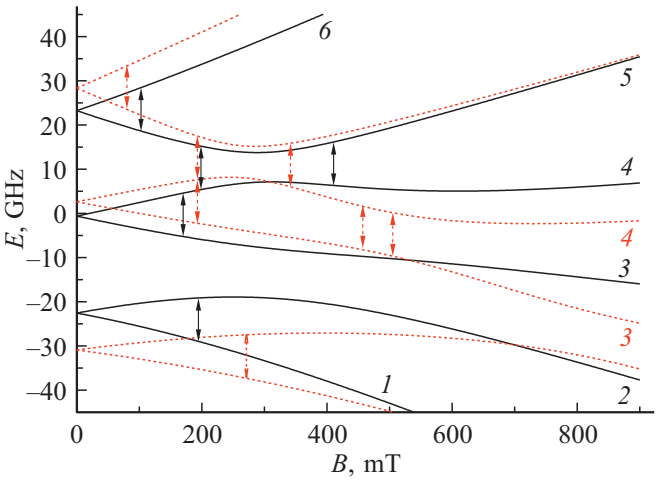

Figure 7. Energy levels and transitions of Fe 1 centers (black solid lines) and Fe 2 (red dashed lines) in Sc_2SiO_5 with **B** ∥ **b** at 9822 MHz.

High rms deviation F(N) at Fe 2 center is evident. Discussion of Figure 7 was focused on the fact that it is Fe 2 center at which many transitions occur between repelling energy levels which results in low accuracy of the used experimental data. Moreover, Figure 6 clearly shows that $dB_{res}/d\theta$ for Fe 2 center is much higher than for Fe 1 center which also results in low accuracy due to orientation error.

Table 2 also shows SH parameters in local coordinate systems of second-rank fine structure tensors where tensors become diagonal with $|b_{20}| > |b_{22}|$. Transition from the laboratory coordinate system to the principal axes system is determined by consecutive rotations using Euler angles (zyz): $\alpha = 349.5$; $\beta = 45.4$; $\gamma = 327.5$ for Fe 1 and $\alpha = 112.2$; $\beta = 285.4$; $\gamma = 166.2$ for Fe 2. The minimum angles between the principal axes Z of these tensors and axis z of the laboratory coordinate system have the following values: $\sim 45°$ for Fe 1 and $\sim 75°$ for Fe 2.

Table 3 shows angles (λ_i) between the principal axes Z of second-rank fine structure tensors of Fe^{3+}, Cr^{3+}, Gd^{3+} centers and axis **z** ∥ **b** in two silicates. In all cases, except gadolinium centers in Sc_2SiO_5, two physically nonequivalent impurity centers with clearly different values λ_i are observed.

The last column lists the centers with lower λ_s, the last but one column lists centers with higher value λ_b. Large difference between λ_i of the iron and chromium centers and λ_i of gadolinium is not surprising, because they belong to different electronic configurations. Moreover, due to substantial difference in ionic radii of Fe^{3+}, Cr^{3+} impurity ions, on the one hand, and of Y^{3+}, Sc^{3+} matrix ions, on the other hand, a considerable relaxation of the paramagnetic defect environment may be expected.

In Section 3, Gd^{3+} center in Sc_2SiO_5 with $\lambda_s = 22°$ is assigned to the gadolinium ion in more spacious position with seven-fold environment (see Table 3). There, more intense Gd^{3+} (Gd 2) center in Y_2SiO_5 with $\lambda_s = 19°$ (taking into account the findings in [20] associated with localization of ^{143}Nd impurity ions in silicates) was assumed as located also in the yttrium position with coordination number 7 (Table 3). Very low concentration of Cr 2 centers with $\lambda_s = 30°$ in Y_2SiO_5 [10] was explained by high mismatch of ionic radii of Cr^{3+} (0.615 Å) and Y^{3+} (0.96 Å) in the seven-fold environment. It can be assumed that angle λ_i is a sign of impurity center localization in two scandium and yttrium positions. To check this assumption, study of Fe^{3+} centers in yttrium silicate crystals is desired.

Table 2. SH parameters of two Fe^{3+} centers in Sc_2SiO_5 in coordinate system **z** ∥ **b** and in the principal axes of the second-rank fine structure tensor. Absolute signs were not determined.

Parameters	Fe 1 **z** ∥ **b**	Fe 1 in principal axes	Fe 2 **z** ∥ **b**	Fe 2 in principal axes
g	2.000	2.000	2.000	2.000
b_{20}	2240	6650	6170	−8990
b_{21}	±18530		∓1060	
b_{22}	5110	6000	6220	6390
c_{21}	±4440		±17680	
c_{22}	−6050		7220	
b_{40}	0	10	−100	−90
b_{41}	±80	−160	∓240	−340
b_{42}	80	−80	350	−240
b_{43}	±230	−650	∓500	300
b_{44}	−250	300	90	−500
c_{41}	±310	−50	±10	30
c_{42}	−210	−140	50	−580
c_{43}	±550	−940	∓1090	0
c_{44}	250	150	−940	−600
F(N)	29(298)		93(430)	

Table 3. Angles between the principal axes Z of second-rank fine structure tensors of Fe^{3+}, Cr^{3+}, Gd^{3+} centers and axis **z** ∥ **b** in two silicates. (Centers with higher intensity are shown in bold. Fe^{3+} spectra in two Sc^{3+} positions and Cr^{3+} position in Sc_2SiO_5 have almost equal intensity.)

Crystal	Ion	$\lambda_b = \angle_b Z\mathbf{z}°$	$\lambda_s = \angle_s Z\mathbf{z}°$
Y_2SiO_5	Cr^{3+} Gd^{3+}	**51** [9,10] 66 [11]	30 [10] **19** [11]
Sc_2SiO_5	Fe^{3+} Cr^{3+} Gd^{3+}	75 herein 68 [12,13] –	45 herein 54 [12,13] **22** [13]
Coordination number		6 ($M1$)	7 ($M2$)

5. Conclusion

Thus, for the purpose of the study, Sc_2SiO_5 : Gd and Sc_2SiO_5 : Fe single-crystals were grown and studied by

the EPR method at 300 K. For the first time, the spin Hamiltonian parameters for two iron(III) centers have been determined on the basis of identified field and orientational dependences of EPR signals in Sc_2SiO_5 crystal.

It has been found that iron(III) ions are included in both nonequivalent crystallographic positions of Sc^{3+} in the crystal structure in comparable quantities. At the same time, Gd^{3+} ions give clear precedence to more spacious position $M2$ with coordination number 7. This result can be adequately explained in terms of the size factor. Analysis of principal axes orientation of the second-rank fine structure tensors suggested that they might by used to determine impurity ion localization.

These findings allow to further detect, by non-destructive EPR methods, foreign microimpurities (1 ppm and lower) of these ions in Sc_2SiO_5 and crystals isostructural to it, which are promising for application as laser and scintillation media as well as in cybernetics.

Funding

The study was financially supported by the Ministry of Science and Higher Education of the Russian Federation, topic No. FEUZ-2023-0017 using the equipment provided by Ural Common Use Center „Modern Nanotechnologies“ Ural Federal University (Reg. No. 2968) supported by the Ministry of Science and Higher Education of the Russian Federation (project 075-15-2021-677).

Conflict of interest

The authors declare that they have no conflict of interest.

References

[1] D.D. Kramushchenko, I.V. Il'in, V.A. Soltamov, P.G. Baranov, V.P. Kalinushkin, M.I. Studenikin, V.P. Danilov, N.N. Il'ichev, P.V. Shapkin. FTT **55**, *2*, 234 (2013). (in Russian).
[2] B.H.T. Chai, Y. Simony, C. Deka, X.X. Zhang, E. Munin, M. Bass. OSA Proc. ASSL **13**, 28 (1992).
[3] Chih-Kang Chang, Jih-Yuan Chang, Yen-Kuang Kuo. Proc. SPIE **4914**, 498 (2002).
[4] L. Zheng, J. Xu, L. Su, H. Li, W. Ryba-Romanowski, R. Lisiecki, P. Solarz. Appl. Phys. Lett. **96**, 121908 (2010).
[5] X. Yang, E. Song, W. Xie. Infrared Phys. Technol. **85**, 154 (2017).
[6] A.L. Alexander, J.J. Longdell, M.J. Sellars, J. Opt. Soc. Am. B **2**, 79 (2007).
[7] R.R. Rakhimov, H.D. Horton, D.E. Jones, G.B. Loutts, H.R. Ries. Chem. Phys. Lett. **319**, 639 (2000).
[8] V.A. Vazhenin, A.P. Potapov, G.S. Shakurov, A.V. Fokin, M.Yu. Artemov, V.A. Isaev. FTT **60**, *10*, 1995 (2018). (in Russian).
[9] V.F. Tarasov, I.V. Yatsyk, R.F. Likerov, A.V. Shestakov, R.M. Eremina, Yu.D. Zavartsev, S.A. Kutovoi. Opt. Mater. **105**, 109913 (2020).
[10] V.A. Vazhenin, A.P. Potapov, K.A. Subbotin, D.A. Lis, M.Yu. Artyomov, V.V. Sanina, E.V. Chernova, A.V. Fokin. Opt. Mater. **117**, 111107 (2021).
[11] A.V. Fokin, V.A. Vazhenin, A.P. Potapov, M.Yu. Artyomov, K.A. Subbotin, A.I. Titov. Opt. Mater. **132**, 112741 (2022).
[12] V.F. Tarasov, R.M. Eremina, K.B. Konov, R.F. Likerov, A.V. Shestakov,Yu.D. Zavartsev, S.A. Kutovoi. Appl. Magn. Res. **52**, 5 (2021).
[13] V.A. Vazhenin, A.P. Potapov, A.V. Fokin, M.Yu. Artemov, V.A. Isaev. FTT **64**, *8*, 967 (2022). (in Russian).
[14] Maria D. Alba, Pablo Chain, Triana Gonzalez-Carrascosa. J. Am. Ceram. Soc. **92**, 487 (2009).
[15] S.A. Altshuler, B.M. Kozyrev. Elektronnyi paramagnitnyi rezonans soedineniy elementov promezhutochnykh grupp. Nauka, M., (1972). P. 121. (in Russian).
[16] R.D. Shannon, Acta Crystallogr., Sect. A: Cryst. Phys., Diffr., Theor. Gen. Crystallogr. **32**, 751 (1976).
[17] R. Eremina, T. Gavrilova, I. Yatsyk, I. Fazlizhanov, R. Likerov, V. Shustov, Yu. Zavartsev, A. Zagumennyi, S. Kutovoi. J. Magn. Magn. Mater. **440**, 13 (2017).
[18] A.A. Sukhanov, V.F. Tarasov, R.M. Eremina, I.V. Yatsyk, R.F. Likerov, A.V. Shestakov, Yu.D. Zavartsev, A.I. Zagumennyi, S.A. Kutovoi. Appl. Magn. Res. **48**, 589 (2017).
[19] R.M. Eremina, V.F. Tarasov, K.B. Konov, T.P. Gavrilova, A.V. Shestakov, V.A. Shustov, S.A. Kutovoi, Yu.D. Zavartsev. Appl. Magn. Res. **49**, 53 (2018).
[20] A.A. Sukhanov, R.F. Likerov, R.M. Eremina, I.V. Yatsyk, T.P. Gavrilova, V.F. Tarasov, Yu.D. Zavartsev, S.A. Kutovoi. J. Magn. Res. **295**, 12 (2018).
[21] I.N. Kurkin, K.P. Chernov. Physica B **101**, 233 (1980).
[22] J.A. Hodges, J.L. Dorman, H. Makram. Phys. Status. Solidi **35**, 53 (1969).

Translated by E.Ilyinskaya